Received: 21 May 2020 | Accepted: 1 June 2020
DOI: 10.1002/pip.3303

ACCELERATED PUBLICATION

PROGRESS IN PHOTOVOLTAICS WILEY

Solar cell efficiency tables (version 56)

Martin A. Green[1] | Ewan D. Dunlop[2] | Jochen Hohl-Ebinger[3] | Masahiro Yoshita[4] | Nikos Kopidakis[5] | Xiaojing Hao[1]

[1]School of Photovoltaic and Renewable Energy Engineering, Australian Centre for Advanced Photovoltaics, University of New South Wales Sydney, Kensington, New South Wales, 2052, Australia

[2]Energy, Transport and Climate, European Commission – Joint Research Centre, Via E. Fermi 2749, Varese, IT-21027, Italy

[3]Department of Characterisation and Simulation/CalLab Cells, Fraunhofer-Institute for Solar Energy Systems, Heidenhofstr. 2, Freiburg, D-79110, Germany

[4]Renewable Energy Research Center (RENRC), National Institute of Advanced Industrial Science and Technology (AIST), Central 2, Umezono 1-1-1, Tsukuba, Ibaraki, 305-8568, Japan

[5]Solar Energy Research Facility (SERF), National Renewable Energy Laboratory, 15013 Denver West Parkway, Golden, CO, 80401, USA

Correspondence
Martin A. Green, School of Photovoltaic and Renewable Energy Engineering, University of New South Wales Sydney, Kensington, New South Wales 2052, Australia.
Email: m.green@unsw.edu.au

Funding information
New Energy and Industrial Technology Development Organization, Grant/Award Number: General; U.S. Department of Energy (Office of Science, Office of Basic Energy Sciences and Energy Efficiency and Renewable Energy, Solar Energy Technology Program), Grant/Award Number: Contract No. DE-AC36-08-GO28308

Abstract

Consolidated tables showing an extensive listing of the highest independently confirmed efficiencies for solar cells and modules are presented. Guidelines for inclusion of results into these tables are outlined, and new entries since January 2020 are reviewed.

KEYWORDS
energy conversion efficiency, photovoltaic efficiency, solar cell efficiency

1 | INTRODUCTION

Since January 1993, "Progress in Photovoltaics" has published six monthly listings of the highest confirmed efficiencies for a range of photovoltaic cell and module technologies.[1–3] By providing guidelines for inclusion of results into these tables, this not only provides an authoritative summary of the current state-of-the-art but also encourages researchers to seek independent confirmation of results and to report results on a standardised basis. In version 33 of these tables,[3] results were updated to the new internationally accepted reference spectrum (International Electrotechnical Commission IEC 60904-3, Ed. 2, 2008).

The most important criterion for inclusion of results into the tables is that they must have been independently measured by a recognised test centre listed elsewhere[2] (one new test centre listed in the Appendix of version 55). A distinction is made between three different eligible definitions of cell area: total area, aperture area and designated illumination area, as also defined elsewhere[2] (note that, if

TABLE 1 Confirmed single-junction terrestrial cell and submodule efficiencies measured under the global AM1.5 spectrum (1000 W/m^2) at 25°C (International Electrotechnical Commission [IEC] 60904-3: 2008, ASTM G-173-03 global)

Classification	Efficiency (%)	Area (cm^2)	V_{oc} (V)	J_{sc} (mA/cm^2)	Fill factor (%)	Test Centre (date)	Description
Silicon							
Si (crystalline cell)	26.7 ± 0.5	79.0 (da)	0.738	42.65[a]	84.9	AIST (3/17)	Kaneka, *n*-type rear IBC[4]
Si (DS wafer cell)	**23.8 ± 0.3**	**246.44 (t)**	**0.7087**	**40.88** [b]	**82.2**	**ISFH (12/19)**	**Canadian solar, *n*-type**
Si (thin transfer submodule)	21.2 ± 0.4	239.7 (ap)	0.687[c]	38.50[c,d]	80.3	NREL (4/14)	Solexel (35 μm thick)[5]
Si (thin-film minimodule)	10.5 ± 0.3	94.0 (ap)	0.492[c]	29.7[c,e]	72.1	FhG-ISE (8/07)	CSG solar (<2 μm on glass)[6]
III–V cells							
GaAs (thin film cell)	29.1 ± 0.6	0.998 (ap)	1.1272	29.78[f]	86.7	FhG-ISE (10/18)	Alta Devices[7]
GaAs (multicrystalline)	18.4 ± 0.5	4.011 (t)	0.994	23.2	79.7	NREL (11/95)	RTI, Ge substrate[8]
InP (crystalline cell)	24.2 ± 0.5[g]	1.008 (ap)	0.939	31.15[a]	82.6	NREL (3/13)	NREL[9]
Thin-film chalcogenide							
CIGS (cell) (cd free)	23.35 ± 0.5	1.043 (da)	0.734	39.58[h]	80.4	AIST (11/18)	Solar Frontier[10]
CdTe (cell)	21.0 ± 0.4	1.0623 (ap)	0.8759	30.25[d]	79.4	Newport (8/14)	First solar, on glass[11]
CZTSSe (cell)	11.3 ± 0.3	1.1761 (da)	0.5333	33.57[f]	63.0	Newport (10/18)	DGIST, Korea[12]
CZTS (cell)	10.0 ± 0.2	1.113 (da)	0.7083	21.77[a]	65.1	NREL (3/17)	UNSW[13]
Amorphous/microcrystalline							
Si (amorphous cell)	10.2 ± 0.3[i,g]	1.001 (da)	0.896	16.36[d]	69.8	AIST (7/14)	AIST[14]
Si (microcrystalline cell)	11.9 ± 0.3[g]	1.044 (da)	0.550	29.72[a]	75.0	AIST (2/17)	AIST[15]
Perovskite							
Perovskite (cell)	21.6 ± 0.6[j,k]	1.0235 (da)	1.193	21.64[l]	83.6	CSIRO (6/19)	ANU[16]
Perovskite (minimodule)	**18.0± 0.6**[j,m]	**19.276(da)**	**1.070**[c]	**21.53**[c,b,n]	**78.4**	**Newport (12/19)**	**Microquanta, 7 serial cells**[17]
Dye sensitised							
Dye (cell)	11.9 ± 0.4[o]	1.005 (da)	0.744	22.47[p]	71.2	AIST (9/12)	Sharp[18]
Dye (minimodule)	10.7 ± 0.4[o]	26.55 (da)	0.754[c]	20.19[c,q]	69.9	AIST (2/15)	Sharp, 7 serial cells[19]
Dye (submodule)	8.8 ± 0.3[o]	398.8 (da)	0.697[c]	18.42[c,r]	68.7	AIST (9/12)	Sharp, 26 serial cells[19]
Organic							
Organic (cell)	13.45 ± 0.2[s]	1.023 (da)	0.8422	23.28[l]	68.6	FhG-ISE (6/19)	Uni Potsdam[20]
Organic (minimodule)	12.6 ± 0.2[s]	26.129(da)	0.8315[c]	21.32[c,l]	71.1	FhG-ISE (9/19)	ZAE Bayern (12 cells)[21]
Organic (submodule)	11.7 ± 0.2[s]	203.98 (da)	0.8177[c]	20.68[c,l]	69.3	FhG-ISE (10/19)	ZAE Bayern (33 cells)[21]

Note. Any changes in the table from those previously published are set in bold type.

Abbreviations: AIST, Japanese National Institute of Advanced Industrial Science and Technology; (ap), aperture area; CIGS, $CuIn_{1-y}Ga_ySe_2$; a-Si, amorphous silicon/hydrogen alloy; CZTSSe, $Cu_2ZnSnS_{4-y}Se_y$; CZTS, Cu_2ZnSnS_4; (da), designated illumination area; DS, directionally solidified (including mono cast and multicrystalline); FhG-ISE, Fraunhofer Institut für Solare Energiesysteme; nc-Si, nanocrystalline or microcrystalline silicon; NREL, National Renewable Energy Laboratory; (t), total area.

[a]Spectral response and current–voltage curve reported in version 50 of these tables.

[b]Spectral response and current–voltage curve reported in the present version of these tables.

[c]Reported on a 'per cell' basis.

[d]Spectral responses and current–voltage curve reported in version 45 of these tables.

[e]Recalibrated from original measurement.

[f]Spectral response and current–voltage curve reported in the version 53 of these tables.

[g]Not measured at an external laboratory.

[h]Spectral response and current–voltage curve reported in version 54 of these tables.

[i]Stabilised by 1000-h exposure to one sun light at 50°C.

[j]Initial performance.

[k]Average of forward and reverse sweeps at 150 mV/s (hysteresis ±0.26%).

[l]Spectral response and current–voltage curve reported in version 55 of these tables.

[m]Measured using 13-point IV sweep with constant bias until data constant at 0.05% level.

[n]Spectral response and current–voltage curve reported in version 52 of these tables.
[o]Initial efficiency. Krašovec et al.[22] review the stability of similar devices.
[p]Spectral response and current–voltage curve reported in version 41 of these tables.
[q]Spectral response and current–voltage curve reported in version 46 of these tables.
[r]Spectral response and current–voltage curve reported in version 43 of these tables.
[s]Initial performance. Tanenbaum et al. and Krebs [23,24] review the stability of similar devices.

masking is used, masks must have a simple aperture geometry, such as square, rectangular or circular). 'Active area' efficiencies are not included. There are also certain minimum values of the area sought for the different device types (above 0.05 cm^2 for a concentrator cell, 1 cm^2 for a one-sun cell, 800 cm^2 for a module and 200 cm^2 for a 'submodule').

Results are reported for cells and modules made from different semiconductors and for subcategories within each semiconductor grouping (e.g., crystalline, polycrystalline and thin film). From version 36 onwards, spectral response information is included (when possible) in the form of a plot of the external quantum efficiency (EQE) versus wavelength, either as absolute values or normalised to the peak measured value. Current–voltage (IV) curves have also been included where possible from version 38 onwards. A graphical summary of progress over the first 25 years during which the tables have been published has been included in version 51.[2]

Highest confirmed 'one sun' cell and module results are reported in Tables 1–4. Any changes in the tables from those previously published[1] are set in bold type. In most cases, a literature reference is provided that describes either the result reported or a similar result (readers identifying improved references are welcome to submit to the lead author). Table 1 summarises the best-reported measurements for one-sun (non-concentrator) single-junction cells and submodules.

Table 2 contains what might be described as 'notable exceptions' for one-sun single-junction cells and submodules in the above category. While not conforming to the requirements to be recognised as a class record, the devices in Table 2 have notable characteristics that will be of interest to sections of the photovoltaic community, with entries based on their significance and timeliness. To encourage discrimination, the table is limited to nominally 12 entries with the present authors having voted for their preferences for inclusion. Readers who have suggestions of notable exceptions for inclusion into this or subsequent tables are welcome to contact any of the authors with full details. Suggestions conforming to the guidelines will be included on the voting list for a future issue.

Table 3 was first introduced in version 49 of these tables and summarises the growing number of cell and submodule results involving high-efficiency, one-sun multiple-junction devices (previously reported in Table 1). Table 4 shows the best results for one-sun modules, both single junction and multiple junctions, while Table 5 shows the best results for concentrator cells and concentrator modules. A small number of notable exceptions are also included in Tables 3–5.

2 | NEW RESULTS

Eight new results are reported in the present version of these tables. The first new result in Table 1 ('one-sun cells') is 23.8% efficiency for a large area (246 cm^2) cell fabricated upon an *n*-type directionally solidified (DS) wafer (commonly called a 'cast mono' wafer), with the cell fabricated by Canadian Solar[70] and the result confirmed by the Institute für Solarenergieforschung (ISFH). The broader 'DS wafer' category displaces the earlier 'multicrystalline' category. Apart from challenges in defining and identifying multicrystallinity, to paraphrase a representative of one major wafer supplier,[71] rather than the present competition being between monocrystalline and multicrystalline products, it is now between the ingot casting process (DS) and the Czochralski growth process.

The second new result in Table 1 is a new efficiency record for a perovskite minimodule. An efficiency of 18.0% is reported for a 19-cm^2minimodule fabricated by Microquanta Semiconductor[18] and measured at the Newport PV Laboratory. For perovskite cells, the tables now accept results based on "quasi-steady-state" measurements (sometimes called "stabilized" in the perovskite field, although this conflicts with usage in other areas of photovoltaics). Along with other emerging technologies, perovskite cells may not demonstrate the same level of stability as conventional cells, with references given below. Five new results are reported in Table 3 relating to one-sun, multijunction devices, three for devices involving Pb-halide perovskites as the top cell material but with three different materials for the bottom cell. . The first new result is for a 4-cm^2 monolithic, 2-junction, 2-terminal GaAsP/Si tandem device fabricated by a joint effort of Ohio State University (OSU), the University of New South Wales, Sydney (UNSW) and SolAero Technologies Corporation and measured at the US National Renewable Energy Laboratory (NREL). The first of the new perovskite results is 29.15% efficiency for a 1-cm^2 perovskite/silicon monolithic two-junction, two-terminal device fabricated by Hemholtz Centrum Berlin (HZB)[72] and measured by the Fraunhofer Institute for Solar Energy Systems (FhG-ISE). This efficiency pushes further beyond the highest efficiency for a single-junction silicon cell (Table 1) with a 9% relative advantage, although for a much smaller area device.

The third new result in Table 3 is for a cell fabricated by the same group (HZB) and measured by the same institute (FhG-ISE) but uses CIGS ($CuIn_xGa_{1-x}Se_2$) as the bottom cell material making it an all thin-film device. An efficiency of 24.2% was measured for a 1-cm^2 perovskite/CIGS monolithic two-junction, two-terminal device,[73] now

TABLE 2 'Notable exceptions' for single-junction cells and submodules: 'Top dozen' confirmed results, not class records, measured under the global AM1.5 spectrum (1000 Wm^{-2}) at 25°C (International Electrotechnical Commission [IEC] 60904-3: 2008, ASTM G-173-03 global)

Classification	Efficiency (%)	Area (cm^2)	V_{oc} (V)	J_{sc} (mA/cm^2)	Fill factor (%)	Test Centre (date)	Description
Cells (silicon)							
Si (crystalline)	26.0 ± 0.5[a]	4.015 (da)	0.7323	42.05[b]	82.3	FhG-ISE (11/19)	FhG-ISE, *p*-type top/rear contacts[25]
Si (crystalline)	25.8 ± 0.5[a]	4.008 (da)	0.7241	42.87[c]	83.1	FhG-ISE (7/17)	FhG-ISE, n-type top/rear contacts[26]
Si (crystalline)	26.1 ± 0.3[a]	3.9857 (da)	0.7266	42.62[d]	84.3	ISFH (2/18)	ISFH, p-type rear IBC[27]
Si (large crystalline)	25.1 ± 0.4	244.45 (t)	0.7470	39.55[b]	85.0	ISFH (9/19)	Hanergy, n-type top/rear contacts[28]
Si (large crystalline)	26.6 ± 0.5	179.74 (da)	0.7403	42.5[e]	84.7	FhG-ISE (11/16)	Kaneka, n-type rear IBC[4]
Si (DS wafer)	22.8 ± 0.3	246.7 (t)	0.6871	40.90[b]	81.2	ISFH (9/19)	Canadian solar, p-type PERC[29]
Cells (III–V)							
GaInP	22.0 ± 0.3[a]	0.2502 (ap)	1.4695	16.63[f]	90.2	NREL (1/19)	NREL, rear HJ, strained AlInP[30]
Cells (chalcogenide)							
CdTe (thin film)	22.1 ± 0.5	0.4798 (da)	0.8872	31.69[g]	78.5	Newport (11/15)	First Solar on glass[31]
CZTSSe (thin film)	12.6 ± 0.3	0.4209 (ap)	0.5134	35.21[h]	69.8	Newport (7/13)	IBM solution grown[32]
CZTS (thin film)	11.0 ± 0.2	0.2339(da)	0.7306	21.74[e]	69.3	NREL (3/17)	UNSW on glass[33]
Cells (other)							
Perovskite (thin film)	25.2 ± 0.8[i,j]	0.0937 (ap)	1.1805	25.14[b]	84.8	Newport (7/19)	KRICT/MIT[34]
Organic (thin film)	17.35 ± 0.2[k]	0.032 (da)	0.862	25.83[b]	78.0	NREL (10/19)	SJTU/UMass[35]
Dye sensitised	12.25 ± 0.4[l,j]	0.0963 (ap)	1.0203	15.17[b]	79.1	Newport (8/19)	EPFL[36]

Abbreviations: AIST, Japanese National Institute of Advanced Industrial Science and Technology; (ap), aperture area; CIGSSe, CuInGaSSe; CZTSSe, $Cu_2ZnSnS_{4-y}Se_y$; CZTS, Cu_2ZnSnS_4; (da), designated illumination area; DS, directionally solidified (including mono cast and multicrystalline); FhG-ISE, Fraunhofer-Institut für Solare Energiesysteme; ISFH, Institute for Solar Energy Research, Hamelin; NREL, National Renewable Energy Laboratory; (t), total area.

[a]Not measured at an external laboratory.
[b]Spectral response and current–voltage curves reported in version 55 of these tables.
[c]Spectral response and current–voltage curves reported in version 51 of these tables.
[d]Spectral response and current–voltage curve reported in version 52 of these tables.
[e]Spectral response and current–voltage curves reported in version 50 of these tables.
[f]Spectral response and current–voltage curve reported in version 54 of these tables
[g]Spectral response and/or current–voltage curves reported in version 46 of these tables.
[h]Spectral response and current–voltage curves reported in version 44 of these tables.
[i]Stability not investigated.
[j]Measured using 10-point IV sweep with constant voltage bias until current determined as unchanging.
[k]Long-term stability not investigated.
[l]Long-term stability not investigated. Krašovec et al.[23] document stability of similar devices.

4% higher than that measured for the best CIGS cell (Table 1). The third new result is for an all-perovskite device. An efficiency also of 24.2% was measured for a 1-cm^2 perovskite/perovskite two-junction, two-terminal device fabricated by Nanjing University[74] and measured by the Japan Electrical Safety and Environment Technology Laboratories (JET). The efficiency is 12% higher than the highest efficiency perovskite cell of similar size in Table 1 (smaller area cells in Table 2 have their efficiency inflated by avoiding series resistance and other compromises normally required in practical devices).

As for other emerging technologies, Pb-halide perovskite cells such as those used as the top cells in these three devices may not

TABLE 3 Confirmed multiple-junction terrestrial cell and submodule efficiencies measured under the global AM1.5 spectrum (1000 W/m^2) at 25°C (International Electrotechnical Commission [IEC] 60904-3: 2008, ASTM G-173-03 global)

Classification	Efficiency (%)	Area (cm^2)	Voc (V)	Jsc (mA/cm^2)	Fill factor (%)	Test centre (date)	Description
III–V multijunctions							
5 junction cell (bonded) (2.17/1.68/1.40/1.06/.73 eV)	38.8 ± 1.2	1.021 (ap)	4.767	9.564	85.2	NREL (7/13)	Spectrolab, 2-terminal[37]
InGaP/GaAs/InGaAs	37.9 ± 1.2	1.047 (ap)	3.065	14.27[a]	86.7	AIST (2/13)	Sharp, 2 term.[38]
GaInP/GaAs (monolithic)	32.8 ± 1.4	1.000 (ap)	2.568	14.56[b]	87.7	NREL (9/17)	LG Electronics, 2 term.
Multijunctions with c-Si							
GaInP/GaAs/Si (mech. stack)	35.9 ± 0.5[c]	1.002 (da)	2.52/0.681	13.6/11.0	87.5/78.5	NREL (2/17)	NREL/CSEM/EPFL, 4-term.[39]
GaInP/AlGaAs/Si (wafer bonded)	34.1 ± 1.2[c]	3.987 (ap)	3.177	12.4[d]	86.4	FhG-ISE (8/19)	Fraunhofer ISE, 2-term.[40]
GaInP/GaAs/Si (monolithic)	24.3 ± 0.9[c]	3.987 (ap)	2.662	12.2[d]	74.5	FhG-ISE (6/19)	Fraunhofer ISE, 2-term.[41]
GaAsP/Si (monolithic)	**23.4±0.3[c]**	**1.026(ap)**	**1.732**	**17.34[e]**	**77.7**	**NREL (5/20)**	**OSU/UNSW/SolAero, 2-term.[42]**
GaAs/Si (mech. stack)	32.8 ± 0.5[c]	1.003 (da)	1.09/0.683	28.9/11.1[e]	85.0/79.2	NREL (12/16)	NREL/CSEM/EPFL, 4-term.[39]
Perovskite/Si (2-terminal)	**29.15 ± 0.7[f]**	**1.060 (da)**	**1.897**	**19.75 [g]**	**77.8**	**FhG-ISE (1/20)**	**HZB[77]**
GaInP/GaInAs/Ge; Si (spectral split minimodule)	34.5 ± 2.0	27.83 (ap)	2.66/0.65	13.1/9.3	85.6/79.0	NREL (4/16)	UNSW/Azur/Trina, 4-term.[43]
Other multijunctions							
Perovskite/CIGS	**24.2 ± 0.7[f]**	**1.045 (da)**	**1.768**	**19.24 [g]**	**72.9**	**FhG-ISE (1/20)**	**HZB, 2-terminal[73]**
Perovskite/perovskite	**24.2 ± 0.8[f]**	**1.041(da)**	**1.986**	**15.93 [g]**	**76.6**	**JET (12/19)**	**Nanjing U, 2-term.[74]**
a-Si/nc-Si/nc-Si (thin film)	14.0 ± 0.4[h,c]	1.045 (da)	1.922	9.94[i]	73.4	AIST (5/16)	AIST, 2-term.[44]
a-Si/nc-Si (thin-film cell)	12.7 ± 0.4[h,c]	1.000(da)	1.342	13.45[j]	70.2	AIST (10/14)	AIST, 2-term.[45]
Notable exceptions							
GaInP/GaAs	**32.9 ± 0.5[c]**	**0.250 (ap)**	**2.500**	**15.36[g,k]**	**85.7**	**NREL (1/20)**	**NREL, multiple QW [77]**
GaInP/GaAs/GaInAs	37.8 ± 1.4	0.998 (ap)	3.013	14.60[k]	85.8	NREL (1/18)	Microlink (ELO)[46]
6 junction (monolithic) (2.19/1.76/1.45/1.19/.97/.7 eV)	39.2 ± 3.2[c]	0.247 (ap)[l]	5.549	8.457[g]	83.5	NREL (11/18)	NREL, inv. metamorphic[47]

Note. Any changes in the table from those previously published are set in bold type.

Abbreviations: a-Si, amorphous silicon/hydrogen alloy; AIST, Japanese National Institute of Advanced Industrial Science and Technology; (ap), aperture area; (da), designated illumination area; ELO, epitaxial lift-off; FhG-ISE, Fraunhofer Institut für Solare Energiesysteme; nc-Si, nanocrystalline or microcrystalline silicon; NREL, National Renewable Energy Laboratory; (t), total area.

[a]Spectral response and current–voltage curve reported in version 42 of these tables.

[b]Spectral response and current–voltage curve reported in the version 51 of these tables.

[c]Not measured at an external laboratory.

[d]Spectral response and current–voltage curve reported in the present version of these tables.

[e]Spectral response and current–voltage curve reported in version 52 of these tables.

[f]Initial efficiency.

[g]Spectral response and current–voltage curve reported in the present version of these tables.

[h]Stabilised by 1000-h exposure to one sun light at 50°C.

[i]Spectral response and current–voltage curve reported in version 49 of these tables.

[j]Spectral responses and current–voltage curve reported in version 45 of these tables.

[k]Spectral response and current–voltage curve reported in version 53 of these tables.
[l]Area too small to qualify as outright class record.

TABLE 4 Confirmed terrestrial module efficiencies measured under the global AM1.5 spectrum (1000 W/m^2) at a cell temperature of 25°C (International Electrotechnical Commission [IEC] 60904-3: 2008, ASTM G-173-03 global)

Classification	Effic. (%)	Area (cm^2)	V_{oc} (V)	I_{sc} (A)	FF (%)	Test Centre (date)	Description
Si (crystalline)	24.4 ± 0.5	13 177 (da)	79.5	5.04[a]	80.1	AIST (9/16)	Kaneka (108 cells)[4]
Si (multicrystalline)	20.4 ± 0.3	14 818 (ap)	39.90	9.833[b]	77.2	FhG-ISE (10/19)	Hanwha Q cells (60 cells)[48]
GaAs (thin film)	25.1 ± 0.8	866.45 (ap)	11.08	2.303[c]	85.3	FhG-ISE (11/17)	Alta Devices[49]
CIGS (Cd free)	19.2 ± 0.5	841 (ap)	48.0	0.456[c]	73.7	AIST (1/17)	Solar frontier (70 cells)[50]
CdTe (thin film)	19.0 ± 0.9	23 573 (da)	227.8	2.560[b]	76.6	FhG-ISE (9/19)	First Solar[51]
a-Si/nc-Si (tandem)	12.3 ± 0.3[d]	14 322 (t)	280.1	0.902[e]	69.9	ESTI (9/14)	TEL solar, Trubbach Labs[52]
Perovskite	**17.9 ± 0.5**[f]	**804 (da)**	**58.7**	**0.323** [g]	**70.3**	**AIST (1/20)**	**Panasonic (55 cells)** [78]
Organic	8.7 ± 0.3[h]	802 (da)	17.47	0.569[i]	70.4	AIST (5/14)	Toshiba[53]
Multijunction							
InGaP/GaAs/InGaAs	31.2 ± 1.2	968 (da)	23.95	1.506	83.6	AIST (2/16)	Sharp (32 cells)[54]
Notable exception							
CIGS (large)	18.6 ± 0.6	10 858 (ap)	58.00	4.545[b]	76.8	FhG-ISE (10/19)	Miasole[55]

Note. Any changes in the table from those previously published are set in bold type.
Abbreviations: a-Si, amorphous silicon/hydrogen alloy; a-SiGe, amorphous silicon/germanium/hydrogen alloy; (ap), aperture area; CIGSS, CuInGaSSe; (da), designated illumination area; Effic., efficiency; nc-Si, nanocrystalline or microcrystalline silicon; (t), total area..
[a]Spectral response and current voltage curve reported in version 49 of these tables.
[b]Spectral response and current–voltage curve reported in version 55 of these tables.
[c]Spectral response and current–voltage curve reported in version 50 or 51 of these tables.
[d]Stabilised at the manufacturer to the 2% level following IEC procedure of repeated measurements.
[e]Spectral response and/or current–voltage curve reported in version 46 of these tables.
[f]Initial performance.
[g]Spectral response and current–voltage curve reported in the present version of these tables.
[h]Initial performance.
[i]Spectral response and current–voltage curve reported in version 45 of these tables.

demonstrate the same level of stability as conventional cells, with the stability of such perovskite cells discussed elsewhere.[75,76] For the present devices, the assigned efficiency was based on measuring the steady-state power at a voltage held constant for 5 min.

The final new result for Table 3 is a 'notable exception' because the cell area was too small for classification as an outright record. Efficiency of 32.9% at one sun was measured for a 0.25-cm^2 two-junction, monolithic GaInP/GaAs cell fabricated and measured at the US National Renewable Energy Laboratory.[77] The cells have a strained, higher bandgap window layer in the GaInP cell to increase the absorption and strain-balanced multiple quantum wells in the bottom cell to extend the range of absorption.

There is one new entry in Table 4 ('one-sun modules'). An efficiency of 17.9% was measured for an 802-cm^2 perovskite module fabricated by Panasonic and measured by the Japanese National Institute of Advanced Industrial Science and Technology. This extends the 16.1% result also from Panasonic reported in the previous version of these tables, with earlier efforts by the same team reported elsewhere.[78]

In Table 5 ('concentrator cells and modules'), one entry originally included in version 53 but inadvertently excluded from subsequent versions has been reinstated as a 'notable exception'. An efficiency of 41.4% is again reported for a 122-cm^2 concentrator minimodule consisting of 10 glass achromatic lenses and 10 wafer-bonded GaInP/GaAs, GaInAsP/GaInAs four-junction solar cells fabricated and measured by FhG-ISE.[79] This is the highest efficiency measured for such an interconnected concentrator module.

The EQE spectra for the new silicon cell reported in the present issue of these tables are shown in Figure 1A, with Figure 1B showing the current density–voltage (JV) curves for the same devices. Figure 2A,B shows the corresponding EQE and JV curves for the new multijunction cell results, while Figure 3A,B shows these for the new perovskite module result.

3 | DISCLAIMER

While the information provided in the tables is provided in good faith, the authors, editors and publishers cannot accept direct responsibility for any errors or omissions.

TABLE 5 Terrestrial concentrator cell and module efficiencies measured under the ASTM G-173-03 direct beam AM1.5 spectrum at a cell temperature of 25°C

Classification	Effic. (%)	Area (cm^2)	Intensity[a] (suns)	Test Centre (date)	Description
Single cells					
GaAs	29.3 ± 0.7[b]	0.09359 (da)	49.9	NREL (10/16)	LG Electronics
Si	27.6 ± 1.2[c]	1.00 (da)	92	FhG-ISE (11/04)	Amonix back-contact[56]
CIGS (thin film)	23.3 ± 1.2[d,e]	0.09902 (ap)	15	NREL (3/14)	NREL[57]
Multijunction cells					
AlGaInP/AlGaAs/GaAs/GaInAs(3) (2.15/1.72/1.41/1.17/0.96/0.70 eV)	47.1 ± 2.6[d,f]	0.099 (da)	143	NREL (3/19)	NREL, 6j inv. m'morphic[47]
GaInP/GaAs/GaInAsP/GaInAs	46.0 ± 2.2[g]	0.0520 (da)	508	AIST (10/14)	Soitec/CEA/FhG-ISE 4j bonded[58]
GaInP/GaAs/GaInAs/GaInAs	45.7 ± 2.3[d,h]	0.09709 (da)	234	NREL (9/14)	NREL, 4j monolithic[59]
InGaP/GaAs/InGaAs	44.4 ± 2.6[i]	0.1652 (da)	302	FhG-ISE (4/13)	Sharp, 3j inverted metamorphic[60]
GaInAsP/GaInAs	35.5 ± 1.2[j,d]	0.10031 (da)	38	NREL (10/17)	NREL 2-junction (2j)[61]
Minimodule					
GaInP/GaAs; GaInAsP/GaInAs	43.4 ± 2.4[d,k]	18.2 (ap)	340[l]	FhG-ISE (7/15)	Fraunhofer ISE 4j (lens/cell)[62]
Submodule					
GaInP/GaInAs/Ge; Si	40.6 ± 2.0[k]	287 (ap)	365	NREL (4/16)	UNSW 4j split spectrum[63]
Modules					
Si	20.5 ± 0.8[d]	1875 (ap)	79	Sandia (4/89)[m]	Sandia/UNSW/ENTECH (12 cells)[64]
Three junction (3j)	35.9 ± 1.8[n]	1092 (ap)	N/A	NREL (8/13)	Amonix[65]
Four junction (4j)	38.9 ± 2.5[o]	812.3 (ap)	333	FhG-ISE (4/15)	Soitec[66]
Notable exceptions					
Si (large area)	21.7 ± 0.7	20.0 (da)	11	Sandia (9/90)[k]	UNSW laser grooved[67]
Luminescent Minimodule	7.1 ± 0.2	25 (ap)	2.5[l]	ESTI (9/08)	ECN Petten, GaAs cells[68]
4j Minimodule	**41.4 ± 2.6[d]**	**121.8 (ap)**	**230**	**FhG-ISE (9/18)**	**FhG-ISE, 10 cells[79]**

Note. Any changes in the table from those previously published are set in bold type.

Abbreviations: (ap), aperture area; CIGS, $CuInGaSe_2$; (da), designated illumination area; Effic., efficiency; FhG-ISE, Fraunhofer-Institut für Solare Energiesysteme; NREL, National Renewable Energy Laboratory.

[a]One sun corresponds to direct irradiance of 1000 Wm^{-2}.

[b]Spectral response and current–voltage curve reported in version 50 of these tables.

[c]Measured under a low aerosol optical depth spectrum similar to ASTM G-173-03 direct.[69]

[d]Not measured at an external laboratory.

[e]Spectral response and current–voltage curve reported in version 44 of these tables.

[f]Spectral response and current–voltage curve reported in version 54 of these tables.

[g]Spectral response and current–voltage curve reported in version 45 of these tables.

[h]Spectral response and current–voltage curve reported in version 46 of these tables.

[i]Spectral response and current–voltage curve reported in version 42 of these tables.

[j]Spectral response and current–voltage curve reported in version 51 of these tables.

[k]Determined at International Electrotechnical Commission 62670-1 CSTC reference conditions.

[l]Geometric concentration.

[m]Recalibrated from original measurement.

[n]Referenced to 1000 W/m^2 direct irradiance and 25°C cell temperature using the prevailing solar spectrum and an in-house procedure for temperature translation.

[o]Measured under International Electrotechnical Commission (IEC) 62670-1 reference conditions following the current IEC power rating draft 626703.

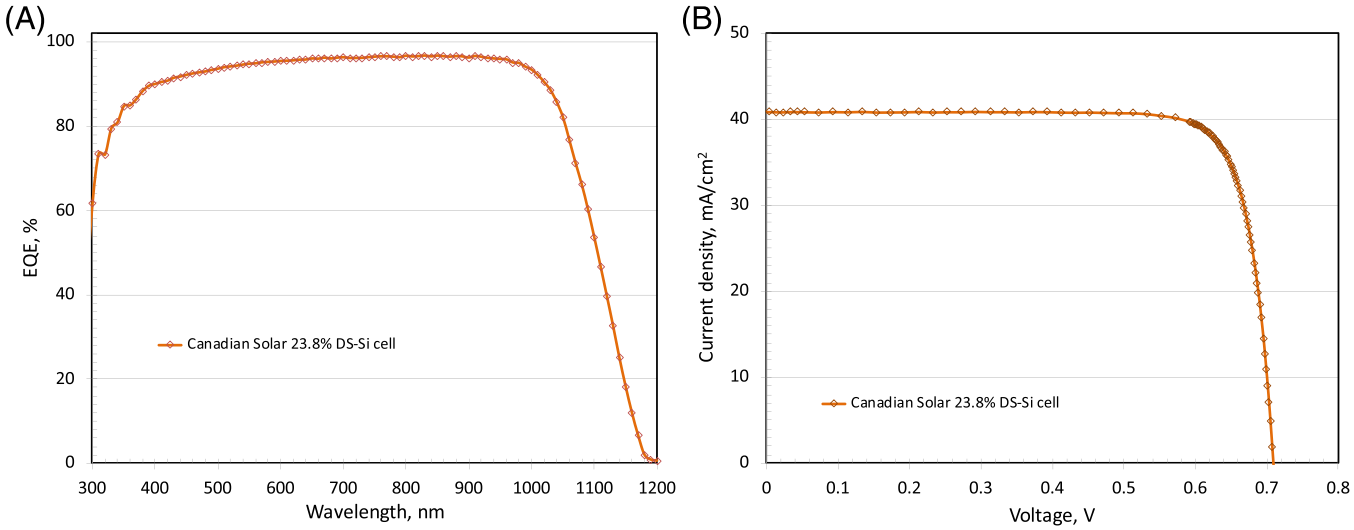

FIGURE 1 A, External quantum efficiency (EQE) for the Si cell reported in this issue (some results may be normalised), B, corresponding current density–voltage (JV) curves [Colour figure can be viewed at wileyonlinelibrary.com]

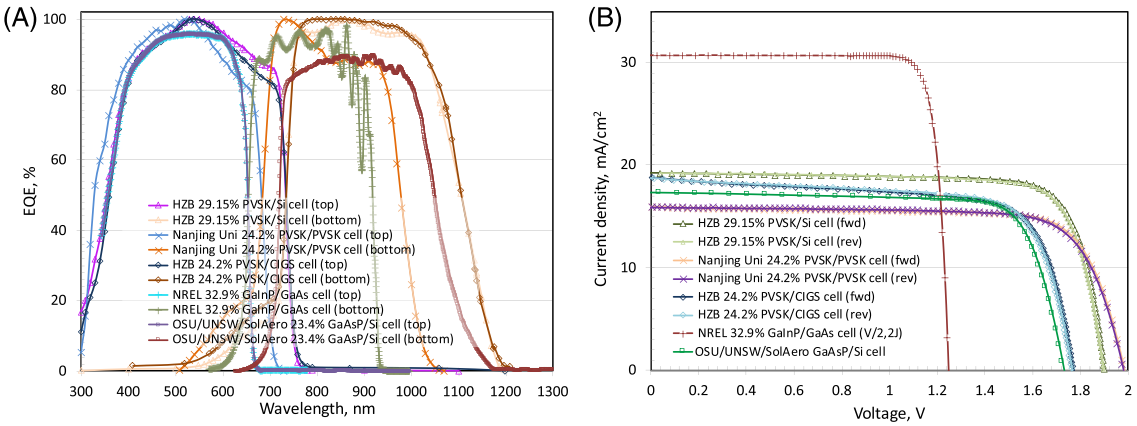

FIGURE 2 A, External quantum efficiency (EQE) for the multijunction cell results reported in this issue (some results may be normalised), B, corresponding current density–voltage (JV) curves [Colour figure can be viewed at wileyonlinelibrary.com]

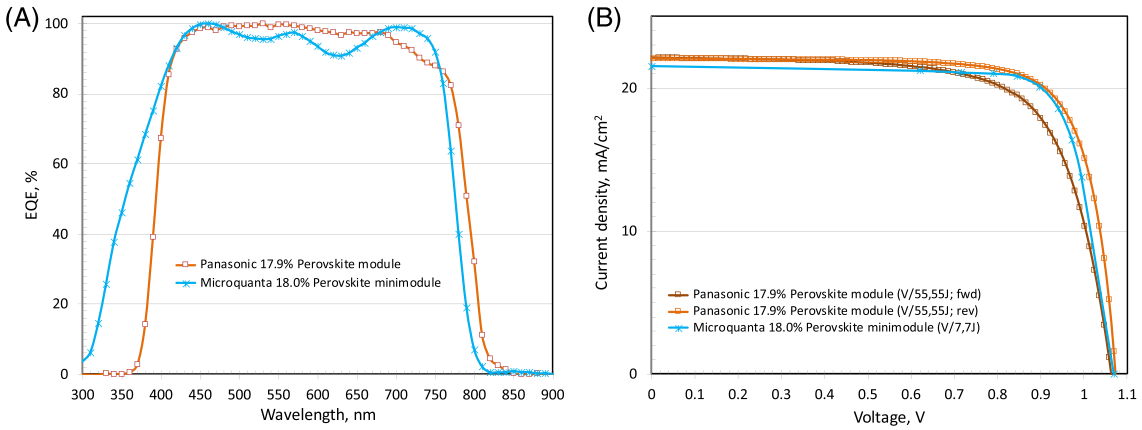

FIGURE 3 A, External quantum efficiency (EQE) for the perovskite module results reported in this issue (some results may be normalised), B, corresponding current density–voltage (JV) curves [Colour figure can be viewed at wileyonlinelibrary.com]

ACKNOWLEDGEMENT

The Australian Centre for Advanced Photovoltaics commenced operation in February 2013 with support from the Australian Government through the Australian Renewable Energy Agency (ARENA). The Australian Government does not accept responsibility for the views, information or advice expressed herein. The work at NREL was supported by the US Department of Energy under Contract No. DE-AC36-08-GO28308 with the National Renewable Energy Laboratory. The work at AIST was supported in part by the Japanese New Energy and Industrial Technology Development Organisation (NEDO) under the Ministry of Economy, Trade and Industry (METI).

ORCID

Martin A. Green https://orcid.org/0000-0002-8860-396X

REFERENCES

1. Green MA, Hishikawa Y, Warta W, et al. Solar cell efficiency tables (version 55). *Progr Photovolt Res Appl*. 2020;28(1):3-15.
2. Green MA, Hishikawa Y, Warta W, et al. Solar cell efficiency tables (version 51). *Progr Photovolt Res Appl*. 2018;26(1):3-12.
3. Green MA, Emery K, Hishikawa Y, Warta W. Solar cell efficiency tables (version 33). *Progr Photovolt Res Appl*. 2009;17(1):85-94.
4. Yoshikawa K, Kawasaki H, Yoshida W, et al. Silicon heterojunction solar cell with interdigitated back contacts for a photoconversion efficiency over 26%. *Nat Energy*. 2017;2(5):17032.
5. Moslehi MM, Kapur P, Kramer J, et al. World-record 20.6% efficiency 156 mm x 156 mm full-square solar cells using low-cost kerfless ultrathin epitaxial silicon & porous silicon lift-off technology for industry-leading high-performance smart PV modules. *PV Asia Pacific Conference (APVIA/PVAP)*, 24 October 2012.
6. Keevers MJ, Young TL, Schubert U, Green MA. 10% efficient CSG minimodules. *22nd European Photovoltaic Solar Energy Conference*, Milan, September 2007.
7. Kayes BM, Nie H, Twist R, Spruytte SG, Reinhardt F, Kizilyalli IC, Higashi GS. 27.6% conversion efficiency, a new record for single-junction solar cells under 1 sun illumination. *Proceedings of the 37th IEEE Photovoltaic Specialists Conference*, 2011.
8. Venkatasubramanian R, O'Quinn BC, Hills JS, et al. 18.2% (AM1.5) efficient GaAs solar cell on optical-grade polycrystalline Ge substrate. *Conference Record, 25th IEEE Photovoltaic Specialists Conference*, Washington, May 1997, 31–36.
9. Wanlass M. Systems and methods for advanced ultra-high-performance InP solar cells. US Patent 9,590,131 B2, 7 March 2017.
10. Nakamura M, Yamaguchi K, Kimoto Y, Yasaki Y, Kato T, Sugimoto H. Cd-free Cu (In,Ga)(Se,S)2 thin-film solar cell with a new world record efficacy of 23.35%, 46th IEEE PVSC, Chicago, IL, June 19, 2019 (see also http://www.solar-frontier.com/eng/news/2019/0117_press.html)
11. First Solar Press Release, First Solar builds the highest efficiency thin film PV cell on record, 5 August 2014.
12. https://en.dgist.ac.kr/site/dgist_eng/menu/984.do (accessed 28 October 2018).
13. Yan C, Huang J, Sun K, et al. $Cu_2ZnSn\ S_4$ solar cells with over 10% power conversion efficiency enabled by heterojunction heat treatment. *Nat Energy*. 2018;3(9):764-772.
14. Matsui T, Bidiville A, Sai H, et al. High-efficiency amorphous silicon solar cells: impact of deposition rate on metastability. *Appl Phys Lett*. 2015;106(5):053901. https://doi.org/10.1063/1.4907001
15. Sai H, Matsui T, Kumagai H, Matsubara K. Thin-film microcrystalline silicon solar cells: 11.9% efficiency and beyond. *Appl Phys Express*. 2018;11(2):022301.
16. https://www.anu.edu.au/news/all-news/anu-researchers-set-solar-record-with-next-gen-cells (accessed 28 October 2019)
17. http://www.microquanta.com (accessed 9 May, 2018).
18. Komiya R, Fukui A, Murofushi N, Koide N, Yamanaka R, Katayama H. Improvement of the conversion efficiency of a monolithic type dye-sensitized solar cell module. *Technical Digest, 21st International Photovoltaic Science and Engineering Conference*, Fukuoka, November 2011; 2C-5O-08.
19. Kawai M. High-durability dye improves efficiency of dye-sensitized solar cells. *Nikkei Electronics* 2013; Feb.1 (http://techon.nikkeibp.co.jp/english/NEWS_EN/20130131/263532/) (accessed 23 October, 2013)
20. https://www.uni-potsdam.de/en/university-of-potsdam.html (accessed 28 October, 2019)
21. https://www.encn.de/fileadmin/user_upload/PR_opv-record__.pdf (accessed 11 November, 2019)
22. Krašovec UO, Bokalič M, Topič M. Ageing of DSSC studied by electroluminescence and transmission imaging. *Solar Energy Mater Solar Cell*. 2013;117:67-72.
23. Tanenbaum DM, Hermenau M, Voroshazi E, et al. The ISOS-3 inter-laboratory collaboration focused on the stability of a variety of organic photovoltaic devices. *RSC Adv*. 2012;2(3):882-893.
24. Krebs FC (Ed). *Stability and Degradation of Organic and Polymer Solar Cells*. Chichester: Wiley; 2012.
25. Zhao J, Wang A, Green MA, Ferrazza F. Novel 19.8% efficient "honeycomb" textured multicrystalline and 24.4% monocrystalline silicon solar cells. *Appl Phys Lett*. 1998;73(14):1991-1993.
26. Richter A, Benick J, Feldmann F, Fell A, Hermle M, Glunz SW. N-type Si solar cells with passivating electron contact: identifying sources for efficiency limitations by wafer thickness and resistivity variation. *Solar Energy Mater Solar Cell*. 2017;173:96-105.
27. Haase F, Klamt C, Schäfer S, et al. Laser contact openings for local poly-Si-metal contacts enabling 26.1%-efficient POLO-IBC solar cells. *Solar Energy Mater Solar Cell*. 2018;186:184-193.
28. http://taiyangnews.info/technology/24-23-shj-thin-film-conversion-efficiency-from-hanergy/ (accessed 28 October 2019).
29. http://investors.canadiansolar.com/news-releases/news-release-details/canadian-solar-sets-2280-conversion-efficiency-world-record-p (accessed 27 October 2019).
30. NREL, private communication, 22 May 2019.
31. First Solar Press Release. First Solar achieves yet another cell conversion efficiency world record, 24 February 2016.
32. Wang W, Winkler MT, Gunawan O, et al. Device characteristics of CZTSSe thin-film solar cells with 12.6% efficiency. *Adv Energy Mater*. 2013;4(7):1301465. https://doi.org/10.1002/aenm.201301465
33. Sun K, Yan C, Liu F, et al. Beyond 9% efficient kesterite Cu_2ZnSnS_4 solar cell: fabricated by using $Zn_{1-x}Cd_xS$ buffer layer. *Adv Energy Mater*. 2016;6(12):1600046. https://doi.org/10.1002/aenm.201600046
34. Jung EH, Jeon NJ, Park EY, et al. Efficient, stable and scalable perovskite solar cells using poly(3-hexylthiophene). *Nature*. 2019;567:511-515.
35. Li ZY, Ying L, Zhu P, et al. A generic green solvent concept boosting the power conversion efficiency of all-polymer solar cells to 11%. *Energ Environ Sci*. 2019;12(1):157-163.
36. https://www.epfl.ch/labs/lspm/; https://www.epfl.ch/labs/lpi/ (accessed 28 October 2019).
37. Chiu PT, Law DL, Woo RL, et al. 35.8% space and 38.8% terrestrial 5J direct bonded cells. *Proc. 40th IEEE Photovoltaic Specialist Conference*, Denver, June 2014; 11–13.
38. Sasaki K, Agui T, Nakaido K, Takahashi N, Onitsuka R, Takamoto T. Proceedings, 9th International Conference on Concentrating Photovoltaics Systems, Miyazaki, Japan 2013.
39. Essig S, Allebé C, Remo T, et al. Raising the one-sun conversion efficiency of III–V/Si solar cells to 32.8% for two junctions and 35.9% for three junctions. *Nat Energy*. 2017;2(9):17144. https://doi.org/10.1038/nenergy.2017.144

40. Cariou R, Benick J, Feldmann F, et al. III-V-on-silicon solar cells reaching 33% photoconversion efficiency in two-terminal configuration. *Nat Energy*. 2018;3(4):326-333. https://doi.org/10.1038/s41560-018-0125-0
41. Feifel M, Lackner D, Ohlmann J, Benick J, Hermle M, Dimroth F. Direct growth of a GaInP/GaAs/Si triple-junction solar cell with 22.3% AM1.5g efficiency. *Sol RRL*. 3(12):1900313. https://doi.org/10.1002/solr.201900313
42. Grassman TJ, Chmielewski DJ, Carnevale SD, Carlin JA, Ringel SA. $GaAs_{0.75}$ $P_{0.25}$/Si dual-junction solar cells grown by MBE and MOCVD. *IEEE J Photovolt*. 2016;6(1):326-331.
43. Green MA, Keevers MJ, Concha Ramon B, et al. Improvements in sunlight to electricity conversion efficiency: above 40% for direct sunlight and over 30% for global. Paper 1AP.1.2, *European Photovoltaic Solar Energy Conference 2015*, Hamburg, September 2015.
44. Sai H, Matsui T, Koida T, Matsubara K. Stabilized 14.0%-efficient triple-junction thin-film silicon solar cell. *Appl Phys Lett*. 2016;109(18):183506. https://doi.org/10.1063/1.49669986
45. Matsui T, Maejima K, Bidiville A, et al. High-efficiency thin-film silicon solar cells realized by integrating stable a-Si: H absorbers into improved device design. *Jpn J Appl Phys*. 2015;54:08KB10. https://doi.org/10.7567/JJAP.54.08KB10
46. http://mldevices.com/index.php/news/ (accessed 28 October 2018).
47. Geisz JF, Steiner MA, Jain N, et al. Building a six-junction inverted metamorphic concentrator solar cell. *IEEE J Photovolt*. 2018;8(2):626-632.
48. https://www.hanwha-qcells.com (accessed 28 October 2019).
49. Mattos LS, Scully SR, Syfu M, et al. New module efficiency record: 23.5% under 1-sun illumination using thin-film single-junction GaAs solar cells. *Proceedings of the 38th IEEE Photovoltaic Specialists Conference*, 2012.
50. Sugimoto H. High efficiency and large volume production of CIS-based modules. *40th IEEE Photovoltaic Specialists Conference*, Denver, June 2014.
51. http://www.firstsolar.com/en-AU/-/media/First-Solar/Technical-Documents/Series-6-Datasheets/Series-6-Datasheet.ashx (accessed 28 October 2019).
52. Cashmore JS, Apolloni M, Braga A, et al. Improved conversion efficiencies of thin-film silicon tandem (MICROMORPH ™) photovoltaic modules. *Solar Energy Mater Solar Cell*. 2016;144:84-95. https://doi.org/10.1016/j.solmat.2015.08.022
53. Hosoya M, Oooka H, Nakao H, et al. Organic thin film photovoltaic modules. *Proceedings of the 93rd Annual Meeting of the Chemical Society of Japan* 2013; 21–37.
54. Takamoto T. Application of InGaP/GaAs/InGaAs triple junction solar cells to space use and concentrator photovoltaic. *40th IEEE Photovoltaic Specialists Conference*, Denver, June 2014.
55. Bheemreddy V, Liu BJJ, Wills A, Murcia CP. Life prediction model development for flexible photovoltaic modules using accelerated damp heat testing. *IEEE 7th World Conference on Photovoltaic Energy Conversion (WCPEC)* 2018: 1249–1251.
56. Slade A, Garboushian V. 27.6% efficient silicon concentrator cell for mass production. *Technical Digest*, 15th International Photovoltaic Science and Engineering Conference, Shanghai, October 2005, 701.
57. Ward JS, Ramanathan K, Hasoon FS, et al. A 21.5% efficient cu (in,Ga)Se_2 thin-film concentrator solar cell. *Progr Photovolt Res Appl*. 2002;10(1):41-46.
58. Dimroth F, Tibbits TND, Niemeyer M, et al. Four-junction wafer-bonded concentrator solar cells. *IEEE J Photovolt*. 2016;6(1):343-349. https://doi.org/10.1109/JPHOTOV.2015.2501729
59. *NREL Press Release NR-4514*, 16 December 2014.
60. Press Release, Sharp Corporation, 31 May 2012 (accessed at http://sharp-world.com/corporate/news/120531.html on 5 June 2013).
61. Jain N, Schulte KL, Geisz JF, et al. High-efficiency inverted metamorphic 1.7/1.1 eV GaInAsP/GaInAs dual-junction solar cells. *Appl Phys Lett*. 2018;112:053905.
62. Steiner M, Siefer G, Schmidt T, Wiesenfarth M, Dimroth F, Bett AW. 43% sunlight to electricity conversion efficiency using CPV. *IEEE J Photovolt*. 2016;6(4):1020-1024. https://doi.org/10.1109/JPHOTOV.2016.2551460
63. Green MA, Keevers MJ, Thomas I, Lasich JB, Emery K, King RR. 40% efficient sunlight to electricity conversion. *Progr Photovolt Res Appl*. 2015;23(6):685-691.
64. Chiang CJ, Richards EH. A 20% efficient photovoltaic concentrator module. *Conf. Record*, 21st IEEE Photovoltaic Specialists Conference, Kissimimee, May 1990: 861–863.
65. http://amonix.com/pressreleases/amonix-achieves-world-record-359-module-efficiency-rating-nrel-4 (accessed 23 October 2013).
66. van Riesen S, Neubauer M, Boos A, et al. New module design with 4-junction solar cells for high efficiencies. *Proceedings of the 11th Conference on Concentrator Photovoltaic Systems*, 2015.
67. Zhang F, Wenham SR, Green MA. Large area, concentrator buried contact solar cells. *IEEE Trans Electron Dev*. 1995;42(1):144-149.
68. Slooff LH, Bende EE, Burgers AR, et al. A luminescent solar concentrator with 7.1% power conversion efficiency. *Phys Stat sol (RRL)*. 2008;2(6):257-259.
69. Gueymard CA, Myers D, Emery K. Proposed reference irradiance spectra for solar energy systems testing. *Solar Energy*. 2002;73(6):443-467.
70. Canadian Solar Press Release, "Canadian solar sets a 23.81% conversion efficiency world record for n-type large area multi-crystalline silicon solar cell", March 6, 2020.
71. http://en.gcl-power.com/news_detail/2403-+New+Era+of+GCL+Cast+Mono+Silicon (Accessed 11 November 2019).
72. Hutchins M. Tandem cells approaching 30% efficiency. PV Magazine, January 30, 2020.
73. https://www.pv-magazine.com/2019/09/11/hzb-hits-23-26-efficiency-with-cigs-perovskite-tandem-cell/ (accessed 28 October 2019).
74. Lin R, Xiao K, Qin ZY, et al. Monolithic all-perovskite tandem solar cells with 24.8% efficiency exploiting comproportionation to suppress Sn (ii) oxidation in precursor ink. *Nat Energy*. 2019;4:864-873.
75. Han Y, Meyer S, Dkhissi Y, et al. Degradation observations of encapsulated planar $CH_3NH_3PbI_3$ perovskite solar cells at high temperatures and humidity. *J Mater Chem a*. 2015;3(15):8139-8147.
76. Yang Y, You J. Make perovskite solar cells stable. *Nature*. 2017;544(7649):155-156.
77. https://www.nrel.gov
78. Higuchi H, Negami T. Largest highly efficient 203 × 203 mm^2 $CH_3NH_3PbI_3$ perovskite solar modules. *Jpn J Appl Phys*. 2018;57:08RE11.
79. Steiner M, Siefer G, Schmidt T, Wiesenfarth M, Dimroth F, Bett AW. 43% sunlight to electricity conversion efficiency using CPV. *IEEE J Photovolt*. July 2016;6(4):1020-1024. https://doi.org/10.1109/JPHOTOV.2016.2551460

How to cite this article: Green MA, Dunlop ED, Hohl-Ebinger J, Yoshita M, Kopidakis N, Hao X. Solar cell efficiency tables (version 56). *Prog Photovolt Res Appl*. 2020;28:629–638. https://doi.org/10.1002/pip.3303